Polymer Degradation and Stability 156 (2018) 43–58

Contents lists available at ScienceDirect

Polymer Degradation and Stability

journal homepage: www.elsevier.com/locate/polydegstab

Rapid mass calorimeter as a high-throughput screening method for the development of flame-retarded TPU

Aleksandra Sut [a], Elke Metzsch-Zilligen [b], Michael Großhauser [b], Rudolf Pfaendner [b], Bernhard Schartel [a, *]

[a] Bundesanstalt für Materialforschung und –prüfung (BAM), Unter den Eichen 87, 12205, Berlin, Germany
[b] Fraunhofer-Institut für Betriebsfestigkeit und Systemzuverlässigkeit LBF, Schlossgartenstr. 6, 64289, Darmstadt, Germany

ARTICLE INFO

Article history:
Received 17 April 2018
Received in revised form
10 July 2018
Accepted 8 August 2018
Available online 10 August 2018

Keywords:
Thermoplastic polyurethane
Flame retardancy
Rapid mass calorimeter
High throughput screening

ABSTRACT

The rapid mass calorimeter (RMC) was used as a screening tool based on accelerated fire testing to assess flame-retarded thermoplastic polyurethane (TPU). The reliability of RMC results was proven with the cone calorimeter as reference fire test. The influence of melamine cyanurate (MC) concentration on the fire performance of TPU was investigated, along with some flame-retardant combinations such as MC with aluminium diethylphosphinate (AlPi), aluminium trihydrate (ATH), and melamine polyphosphate (MPP). The two-stage burning behaviour of TPU was investigated in detail; the first stage corresponds mainly to the hard segments' decomposition and has a much lower effective heat of combustion (EHC) than the second stage, in which mainly the soft segments decompose and an intensive liquid pool fire is observed in the cone calorimeter set-up. In addition to fire testing with the cone calorimeter, RMC, and UL 94 flammability tests, the decomposition of the materials was investigated using thermogravimetric analysis coupled with infrared spectrometry (TG–FTIR). TPU/MC/AlPi shows the most promising results, achieving V-0 classification in UL 94 and reducing the extreme peak heat release rate (PHRR) of the liquid pool fire from 3154 kW/m^2 to 635 kW/m^2. Using MC/AlPi/MPP enhances the latter PHRR reduction further. The decomposition products identified in the gas phase via TG–FTIR reveal specific MC–AlPi –MPP interactions, as they differ from products seen in systems with MC/AlPi or MC/MPP. Correlations between RMC and cone calorimeter results were examined and presented in the final part of the paper. Several characteristics correlate strongly, pointing out that RMC is a reliable high-throughput fire testing method to screen multicomponent flame-retardant solutions in TPU.

© 2018 The Authors. Published by Elsevier Ltd. This is an open access article under the CC BY-NC-ND license (http://creativecommons.org/licenses/by-nc-nd/4.0/).

1. Introduction

Thermoplastic polyurethanes (TPU) are one of the most common classes of thermoplastic elastomers [1]. TPUs are linear copolymers consisting of alternating hard and soft segments. Due to their excellent chemical resistance, as well as good mechanical properties like high tensile strength and abrasion resistance, TPUs are used in variety of applications [2–4], with a strong focus on the cable and wire market. However, TPU is highly flammable; once ignited, it melts and forms liquid pool fires or burning drops, which can cause the ignition of further items and high heat release rates, and thus lead to intensive flame spread. TPU does not meet any of the fire safety requirements imposed for several applications. To reduce the fire risks of TPU is not a trivial task, because very efficient flame retardancy is needed, while the total amount of additives must be kept as low as possible in order to limit deterioration in processing and mechanical properties. The flame retardancy of TPU is a very complex issue and calls for well-elaborated strategies adjusted to the targeted applications.

Flame retardancy approaches for TPU depend on which fire test is considered for the intended application. In the cone calorimeter, for instance, the formation of a liquid pool fire results in a very high peak heat release rate (PHRR) at the end of the burning of TPU. Hence, one of the strategies is the introduction of char-forming additives to limit the formation of liquid pool fires and reduce the PHRR. The flammability tests required for electrical engineering, such as the UL 94 classification, are more contingent on the first burning stage, such that the flame retardants must enhance immediate extinction in reaction to a small flame to achieve non-dripping V-0 or non-flaming dripping V-0 classification.

* Corresponding author.
E-mail address: bernhard.schartel@bam.de (B. Schartel).

https://doi.org/10.1016/j.polymdegradstab.2018.08.004
0141-3910/© 2018 The Authors. Published by Elsevier Ltd. This is an open access article under the CC BY-NC-ND license (http://creativecommons.org/licenses/by-nc-nd/4.0/).

Further, the challenge is to find suitable flame retardants that ensure efficient flame retardancy while meeting the market demand for halogen-free and environmentally friendly solutions. Nowadays combinations based of phosphorus-based and/or nitrogen-rich flame retardants are leading the market among others; e.g. melamine derivatives like melamine cyanurate (MC) and melamine polyphosphate (MPP), along with phosphorous flame retardants like arylphosphates and aluminium diethylphosphinate (AlPi). Several publications have also addressed the use of mineral fillers and intumescent systems, e.g. the addition of aluminium trihydroxide (ATH) or the combination of ammonium polyphosphate (APP) and adjuvants such as iron-graphene synergists [5–7]. High loadings of additives are often required, e.g. 60 wt.-% ATH to achieve V-0, which can have a critical influence on the mechanical properties of the compound [8], but are common solutions in the wire and cable industry. The influence of metal oxides in intumescent flame-retarded TPU systems was reported in the literature as well, e.g. in combination with ammonium pentaborate or with APP [9–11]. An extensive review of flame-retarded polyurethanes was given by Levchik and Weil as well as by Toldy [12,13].

The successful use of MC in combination with other flame retardants and/or adjuvants is crucial, especially applications in cable jackets [7,14]. A prominent phosphorus-based flame retardant is AlPi, which acts mainly as a flame inhibitor in the gas phase. It was reported that addition of 30 wt.-% of AlPi to TPU leads to V-0 classification in the UL 94 test at 3 mm sample thickness [15]. However, recently it was demonstrated that it is much more promising to use smaller amounts of AlPi in synergistic multicomponent systems in highly flammable polymers [16,17]. To sum up, current research and development of modern flame-retardant TPU are focussing on halogen-free multicomponent flame-retardancy approaches.

The plethora of possible variations in multicomponent flame retardant systems demands the use of screening and high-throughput methods in fire testing. Some of the proposed screening methods rely on milligram-based sample testing, e.g. pyrolysis combustion flow calorimeter (PCFC, or microscale combustion calorimeter MCC), which allows the heat release rate of investigated mg-specimens to be monitored upon heating at a constant heating rate [18,19]. Nevertheless, the small sample size and absence of a real flame restrict the assessment of some phenomena like flame inhibition or formation of intumescence/a protective layer. For this reason a new method was proposed recently, namely the rapid mass calorimeter (RMC) [20,21]. In this approach, reduced-size specimens (20 mm × 20 mm) are tested in a modified semi-automated mass loss calorimeter equipped with a linear motion unit and two sample holders, which significantly reduces the amount of material needed and shortens the time of testing.

The RMC is proposed as a fast and reliable screening method for the development of flame-retarded TPU in this study. At first the influence of MC concentration on the flame-retardant properties of TPU is investigated, as well as the combinations of MC with AlPi or ATH. A better understanding of the fire behaviour of flame retarded TPU is provided as well as an insight in the influence of different modes of action. Based on those systems and results, several multicomponent systems were chosen and investigated in terms of fire behaviour and thermal decomposition in the second part of the paper. Mechanical testing was performed as a complementary characterization with respect to application. In addition, to demonstrate the reliability of RMC, the correlations between RMC and cone calorimeter are discussed. The paper proposes the RMC as a reliable high-throughput fire testing method to screen multicomponent flame-retardant solutions and scrutinizes some multicomponent flame-retardant approaches in TPU.

2. Experimental

2.1. Materials

The investigated materials were prepared in two different ways, either by compounding with an extruder followed by injection moulding into the test specimen (method 1), or by extrusion of a band followed by stamping or cutting out the specimen (method 2). Only materials produced using the same method were compared in this study. TPU (Elastollan® 1185A10, BASF SE), as well as TPU with various concentrations of MC (Melapur MC 50, BASF SE) and combinations with 10 wt.-% AlPi (particle size d_{50} 20–40 μm, Exolit OP 1240, Clariant Produkte (Deutschland) GmbH) and 15 wt.-% ATH (Apyral 210, Nabaltec AG) were provided by GRAFE Advanced Polymers GmbH following method 1. The compounds were compounded via twin-screw extrusion (ZSE 27, Leistritz Extrusionstechnik GmbH). The test specimens were prepared via injection moulding. The multicomponent systems investigated in the second part of this study included the previously introduced ingredients, and also contained MPP (Melapur 200, BASF SE), modified layered magnesium aluminium silicate pellets (clay, Cloisite 20B, BYK -Chemie GmbH), silica powder (Si, non-commercial product) and AlPi (particle size d_{50} 25–50 μm, Exolit OP 1230, Clariant Produkte (Deutschland) GmbH). Commercially available halogen-free flame-retarded TPU-FR (Elastollan® 1185A10FHF, BASF SE) was investigated as well as a benchmark. These multicomponent compounds were prepared with a twin-screw extruder (W&P ZSK 18, Coperion GmbH) at the Fraunhofer Institute for Structural Durability and System Reliability LBF. The extruder was coupled with a cast film line (chill roll, Dr. COLLIN GmbH). The materials are directly conveyed from the extruder to the cast film line. Depending on the amount of each compound, the obtained 2–2.1 mm thick films varied in their lengths. The exact composition and preparation methods for all materials are presented in Table 1.

2.2. Fire behaviour

The RMC was used as it was recently proposed as high-throughput screening method [21]. The RMC consists of a mass loss calorimeter (Fire Testing Technology Ltd., FTT) and a chimney equipped with thermocouples to record the heat release rate (HRR) according to ISO 13927. The balance of the mass loss calorimeter was replaced with a linear motion unit (Oriental Motor Co., LTD.) to provide for semi-automatic sample exchange. The specimens were cut into samples 20 mm × 20 mm in size and placed in an aluminium tray. The heat flux was set to 50 kW/m^2 and the distance between the specimen surface and the cone heater was 25 mm. The detailed set-up is described elsewhere [22]. As a reference method the cone calorimeter (Fire Testing Technology Ltd., FTT) was used, which simulates forced-flaming combustion according to ISO 5660. The specimens, 100 mm × 100 mm in size, were investigated at a heat flux of 50 kW/m^2 and with a distance of 35 mm between the cone heater and the sample surface, ensuring proper results and giving the materials some space for moderate intumescence [22]. In both tests the thickness of the specimens was either 3 mm or 2 mm, depending on the material preparation method. For each material two specimens were investigated in RMC and cone calorimeter, respectively. When the deviation exceeded 10% in any important characteristic, a third measurement was performed. For industrial applications, especially in electronics, the flammability (reaction to a small flame) rating of the materials is required according to UL94. Therefore, all materials presented in this study were tested in a vertical UL 94 burning chamber (Fire Testing Technology Ltd., FTT) according to IEC 60695-11-10. The samples were 13 mm wide and 3 mm (method 1) or 2 mm (method 2) thick. Thus, the same

Table 1
Material compositions and preparation method.

Material	Abbreviation	Preparation	Thickness
Elastollan® 1185A10 (TPU)	TPU	Method 1: Extrusion followed by injection moulding into specimen	3 mm
TPU +10 wt.-% Melapur MC 50	TPU/10MC		
TPU +20 wt.-% MC	TPU/20MC		
TPU +30 wt.-% MC	TPU/30MC		
TPU +20 wt.-% MC +10 wt.-% Exolit OP 1240	TPU/20MC/10AlPi		
TPU +15 wt.-% MC +15 wt.-% Apyral 210	TPU/15MC/15ATH		
TPU +10 wt.-% MC +10 wt.-% Melapur 200	TPU/10MC/10MPP	Method 2: Extrusion into thick films	2 −2.1 mm
TPU +9 wt.-% MC +6 wt.-% MPP +15 wt.-% Exolit OP 1230	TPU/9MC/6MPP/15AlPi		
TPU +9 wt.-% MC +6 wt.-% MPP +15 wt.-% AlPi +3 wt.-% Silica	TPU/9MC/6MPP/15AlPi/3Si		
TPU +15 wt.-% MC +15 wt.-% AlPi	TPU/15MC/15AlPi		
TPU +18 wt.-% MC +5 wt.-% Clay	TPU/18MC/5Clay		
Elastollan® 1185A10FHF	TPU-FR		

thickness was used for the test specimen in UL 94, RMC and cone calorimeter.

2.3. Pyrolysis

The decomposition and corresponding mass loss under nitrogen were monitored via thermogravimetric analysis (TG) using a TG 209 F1 Iris (NETZSCH-Gerätebau GmbH). The mass of the specimen investigated was 5 mg; the heating rate was 10 K/min. Evolved gas analysis was done by coupling the TG with a Fourier transform infrared spectroscope (FTIR, Tensor 27, Bruker Corporation) via a heated transfer tube. This transfer line and the gas cell of the FTIR were heated to 260 °C.

2.4. Correlation analysis

The correlation between the RMC and the cone calorimeter results were evaluated based on the Pearson correlation coefficient R. Pearson R values range from ±1 for perfect correlation to 0 for no correlation at all [23].

2.5. Mechanical testing

Mechanical testing was performed for the multicomponent systems in the second part of the paper to complete the comprehensive exploration. The samples for mechanical testing were stamped out of the produced films. The samples were stamped out in the direction of the film production flow. Quasi-static tensile tests were performed at a velocity of $v = 100$ mm/min using a universal tensile testing machine (zwickiLine 2.5, Zwick GmbH & Co.KG) under standard atmosphere according to ISO 291 at 23 °C and 50% RH. For each test configuration, the final result was generated from the average values of five single tests. Each sample was pulled until elongation at break. The tensile strains were measured directly in the lateral and transverse directions using an optical extensometer. In this way the true quantities of stress and strain were obtained and subsequently used to calculate elongation at break and tensile strength.

3. Results and discussion

3.1. Influence of the MC concentration on performance

To investigate the influence of the MC concentration on fire performance, TPU was mixed with 10, 20 and 30 wt.-% MC. Additionally, combination with two potential synergists, AlPi and ATH, was investigated as a first step towards multicomponent systems.

3.1.1. Screening fire performance: rapid mass calorimeter (RMC)

With appropriate programming of the RMC procedure, it was easy to test a series of several samples quickly. As a result, the heat release rate curves seen in Fig. 1 a were obtained. At first glance, each material seems to be represented as a featureless peak, but a closer look reveals certain characteristics like a subtle shoulder preceding the peak. The addition of flame retardants reduced the PHRR, with the strongest effects observed for TPU/30MC and TPU/20MC/10AlPi. The shape of the HRR curve changed most for TPU/15MC/15ATH; the initial shoulder was pronounced, suggesting that ATH affected the polymer decomposition matrix by slowing down the first step (dominated by hard segments decomposition), mainly due to the strong water release at the beginning of burning. By plotting the PHRR over the total heat evolved (THE) (Fig. 1 b) the general fire performance of the flame-retarded materials is assessed, whereby the data points closer to the origin of the plot are considered to be better flame-retardant materials. Further, the flame-retardant effect itself is illustrated when TPU is used as the material for comparison. It was concluded that the most promising material is the combination of flame retardants in TPU/20MC/10AlPi.

Plotting PHRR over MC content revealed an almost linear decrease in PHRR, with increasing amounts of MC in the polymer matrix (Fig. 1 c). The strongest reduction was observed for TPU/30MC, where a broader HRR curve appeared as burning proceeded. When MC was combined with AlPi in TPU/20MC/10AlPi, the PHRR was similar to TPU/30MC, whereas TPU/15MC/15ATH had a PHRR in the range of TPU/20MC.

The analysis of THE gave rather unexpected results for the TPU/MC materials (Fig. 1 d). THE seemed increased with the increase in MC content, in contrast to the expected fuel dilution effect by replacing TPU with MC and the ammonia release of MC. In case of TPU/20MC/10AlPi and TPU/15MC/15AlPi, the THE was lower. Additionally the reduction in THE for TPU/15MC/15ATH was most probably due to the replacement of fuel by ATH according to the vol.-% of ATH, whereas the lowest THE was measured for TPU/20MC/10AlPi, which corresponded with the flame-inhibition effect expected for AlPi.

TPU, TPU/10MC, and TPU/20MC showed hardly any residue after the test (Fig. 1 e); the residues remaining for TPU/30MC and TPU/20MC/10AlPi are somewhat similar, but the different colours of the residues suggest that the nature of TPU/20/10AlPi is closer to carbonaceous char (more black). The fire residue formed for TPU/30MC was not higher than the aluminium foil wrapped around the specimen and its surface was very porous. In case of TPU/20MC/10AlPi the fire residue was slightly higher than then aluminium tray and the surface appeared somewhat denser. The residue of TPU/15MC/15ATH was flat and compact and the white colour suggested mainly inorganic character.

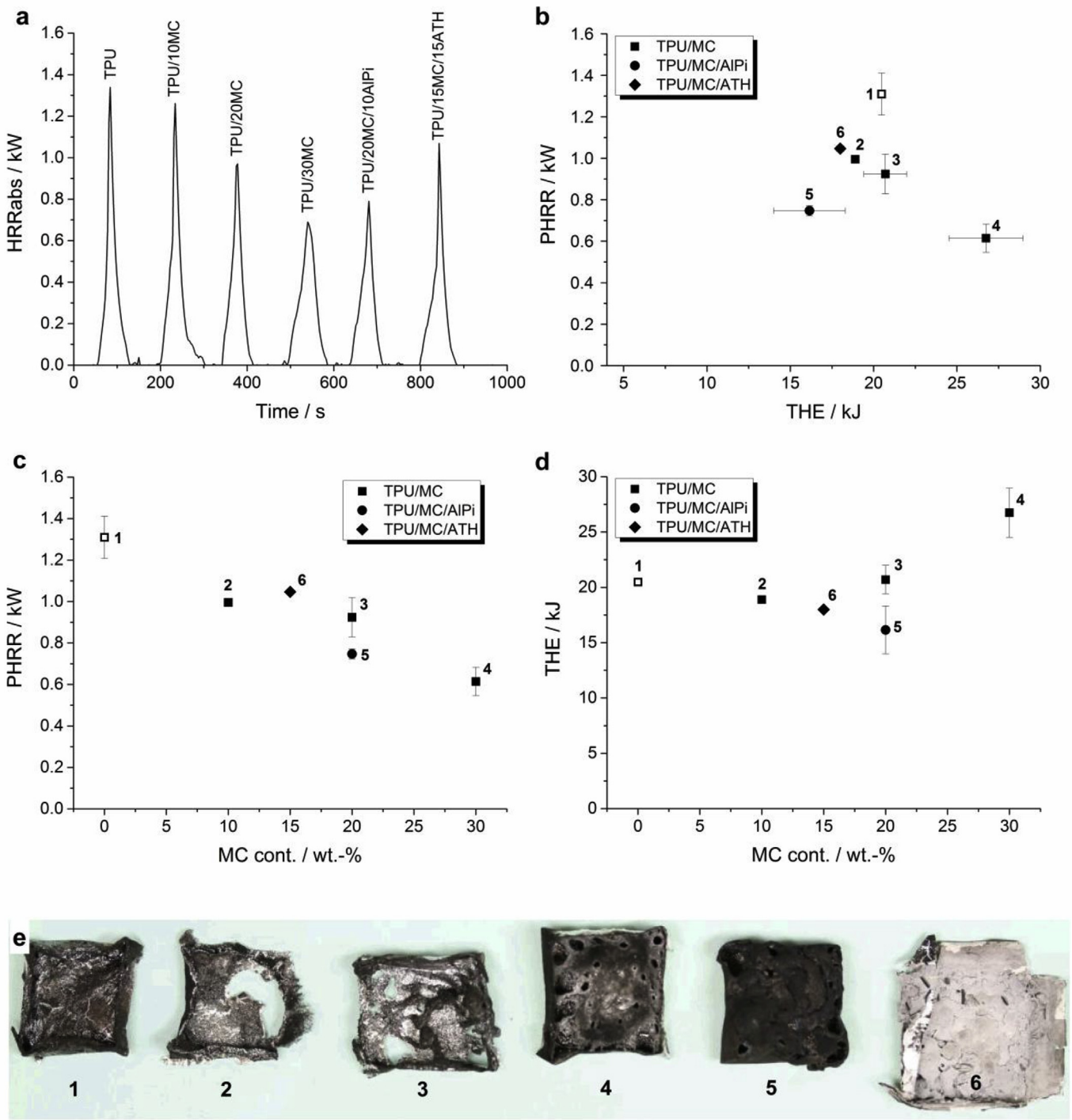

Fig. 1. RMC HRR curves (a), relation between PHRR and THE (b), and influence of MC concentration on PHRR (c) and THE (d); residues after RMC test (d): TPU (1), TPU/10MC (2), TPU/20MC (3), TPU/30MC (4), TPU/20MC/10AlPi (5), TPU/15MC/15ATH (6).

3.1.2. Fire behaviour: cone calorimeter

To characterize the fire behaviour, all materials were investigated in the cone calorimeter. TPU burns in a specific manner due to its chemical structure; it can be considered as a block copolymer with alternating hard (rigid) and soft (flexible) segments. Once exposed to the heat source in the cone calorimeter, the specimens buckled slightly and then softened, which is related not only to a softening of the TPU, but also to the beginning of decomposition of the hard segments. Thus, ignition followed shortly afterward. At first burning was moderate, but as soon as the sample was completely molten, a liquid pool fire was created and the soft segments decomposed. Just before flame-out the material became solid and shrank. In case of the flame-retarded TPU, similar burning behaviour was observed, but for some of the materials several 'char islands' formed on the surface of the boiling liquid.

As presented in Fig. 2, the beginning of the HRR curves was quite similar for all materials, suggesting that the flame retardants did not influence the initial, first stage of burning. The PHRR of TPU

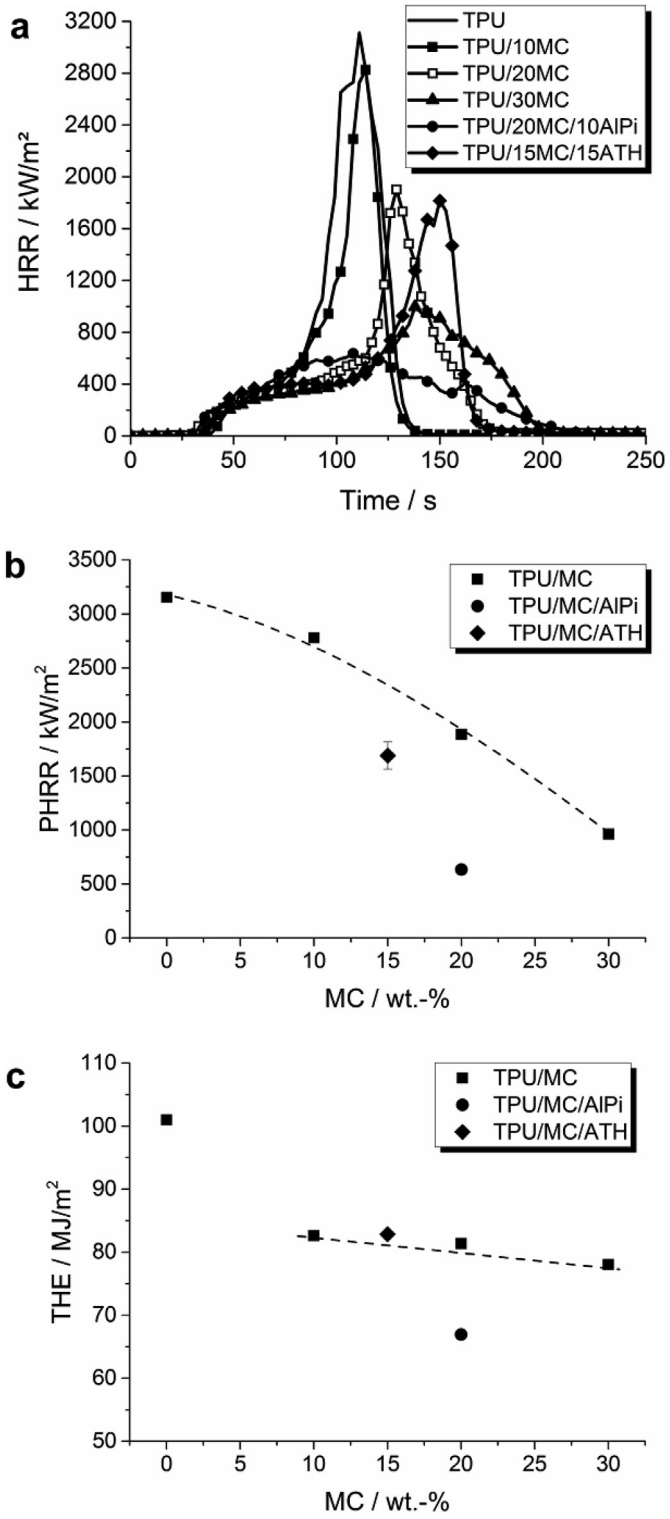

Fig. 2. a) Heat release rate (HRR) curves of TPU, TPU/MC with different MC content, TPU/20MC/10AlPi, and TPU/15MC/15ATH; b) PHRR and c) THE plotted over the MC concentration.

reached a very high 3154 kW/m^2 at the end of burning, and thus the shape is typical for non-charring materials [24]. Addition of 10 wt.-% MC did not improve performance and the PHRR was still very high (2780 kW/m^2). TPU/20MC and TPU/15MC/15ATH presented similar curve shapes as well, i.e. an initial plateau and a peak at the end, but the burning time was prolonged, PHRR reduced, and time to PHRR and burning time also increased. When 30 wt.-% of MC was added to the TPU, there was significant reduction in the PHRR and the shape began to shift towards a char-forming type. A pronounced change in the burning behaviour was observed for TPU/20MC/10AlPi, indicated by the change in the HRR curve shape, including the strongest reduction in PHRR, to 635 kW/m^2. The interpretation of the cone calorimeter results corresponded with the conclusions based on the RMC test.

Detailed analysis of the characteristic cone calorimeter results gave better insight into the influence of MC concentration. The PHRR decreased almost linearly (Fig. 2 b) with increasing MC content; the reduction became somewhat stronger with higher loads of MC. The addition of ATH in TPU/15MC/15ATH caused a much stronger decrease in PHRR, nearly twofold, compared to the PHRR value interpolated for TPU/15MC (Fig. 2 b). The most impressive flame retardancy in PHRR was observed for TPU/20MC/10AlPi, where the PHRR was reduced by 80% in comparison to TPU. The reduction was not only much greater than that observed for TPU/20MC, but also greater than for TPU/30MC. Replacing part of the MC with AlPi yielded better results. The THE values (Fig. 2 c) were comparable for all flame-retarded materials, showing a reduction of ~20%, with the exception of TPU/20MC/10AlPi, which showed a reduction of more than 30% compared to TPU. Thus there was considerable reduction in THE compared to TPU for all flame-retarded materials investigated.

As mentioned before, TPU shows specific burning behaviour. We assumed that the two stages of burning would have different effective heats of combustion according to the change in pyrolysis products. Thus EHC for the complete burning, and EHC_1 and EHC_2 for the both stages, were calculated based on the tangent method applied to the HRR curve, where the onset and offset points were determined and the mean EHC value was calculated for each step (Table 2, Fig. 3). This method worked well for most of the presented systems, as long as the initial burning process was well separated from the subsequent burning stage as a liquid pool fire.

The effective heat of combustion is defined as the amount of heat evolved divided by the mass lost. The first stage had a relatively low EHC_1 (Fig. 3 a) of 23 MJ/kg for TPU. EHC_1 was reduced to around 20 MJ/kg for all flame-retarded materials except TPU/20MC/10AlPi, where the EHC_1 was 16 MJ/kg. Compared to TPU the reduction was considerable. Since the beginning of the HRR curve and thus the THE was almost exactly the same for all materials (see Fig. 3), the difference is related to the increased mass loss. The higher mass loss for flame-retarded materials was due to the interaction with the polymer matrix and the release of additional non-combustible volatiles causing fuel dilution, mainly from the MC decomposition. TPU/15MC/15ATH showed additional fuel dilution due to the water released by ATH. TPU/20MC/10AlPi showed the largest decrease, due to additional flame inhibition caused by AlPi. The second burning stage, the liquid pool-like fire, has a much higher EHC (Fig. 3 b). In this second burning stage the flame inhibition of AlPi was much more pronounced, whereas the other systems showed values similar to TPU. There is no reduction in EHC_2 for TPU/15MC/15ATH because at this point all of the water and ammonia have already been released. The fuel dilution effect of MC and ATH was consumed mainly in the first burning stage, whereas their residue formation in the condensed phase influenced the second burning stage. In contrast, AlPi works as a flame inhibitor in TPU/20MC/10AlPi in the second burning stage as well, releasing phosphorus species and hence reducing the EHC [25,26].

The EHC values averaged over the entire burning time (Fig. 3 c) show a linear decrease with increasing MC content. The two multicomponent systems TPU/15MC/15ATH and TPU/20MC/10AlPi are below this line. The strongest EHC reduction is observed in TPU/20MC/10AlPi, as a result of fuel dilution by MC and the strong flame

Table 2
Cone calorimeter data. PHRR – peak heat release rate; THE – total heat evolved; EHC – effective heat of combustion for the first burning stage (subscript 1), second (subscript 2) and averaged over the entire time of burning.

Name	PHRR kW/m^2	THE MJ/m^2	EHC$_1$ MJ/kg	EHC$_2$ MJ/kg	EHC MJ/kg	Residue %	UL 94 Vertical
TPU	3154	101	23	32	29	2	V-2
TPU/10MC	2780	83	20	24	27	8	V-2
TPU/20MC	1887	81	20	31	26	7	V-2
TPU/30MC	963	78	19	28	24	8	V-2
TPU/20MC/10AlPi	635	67	16	24	20	7	V-0
TPU/15MC/15ATH	1690	83	20	33	25	11	V-2

inhibition of AlPi. Separation into two stages of burning allows the particular flame retardant functions on the EHC to be differentiated in each stage.

Fire performance in the cone calorimeter depends not only on the gas-phase activity underlined by the EHC discussion, but also strongly on the condensed-phase flame-retardancy modes of action. Hence a detailed analysis of the residues was performed to complete the discussion of the fire behaviour of TPU and flame-retarded TPU composites.

TPU formed around 2 wt.-% of loose residue (Fig. 4). The addition of MC in TPU/MC materials improved residue formation, and adding 10, 20 and 30 wt.-% MC yielded a similar amount of residue, between 7 and 8 wt.-%. Adding MC led to the formation of a very porous, thin residue layer (Fig. 4), which seemed to provide a limited protection layer effect, but when MC was combined with AlPi in TPU/20MC/10AlPi, the morphology changed. The residue yield was similar (around 8 wt.- %), but a residue with a layered structure was formed, resulting in better protection properties, which explained the outstanding fire performance in the cone calorimeter, reduction in HRR and change in the shape of the HRR curve. It was reported in the literature that combining MC and aluminium hypophosphite leads to the formation of compact char layer [27]. Some gases evolved seemed to inflate the char slightly, resulting in the formation of the separated inner layers. TPU/15MC/15ATH forms a very dense inorganic-organic layer (Fig. 4). As a result, the PHRR was reduced, but the thermal insulation was not as good as for TPU/20MC/10AlPi.

The flammability (reaction to a small flame) of the materials was evaluated with the UL 94 test. All materials exhibited dripping when the burner was placed under the specimen bar, and extinguished nearly immediately after removing the flame. The drops ignited the cotton so that V-2 classification was reached by TPU, all TPU/MC materials, and TPU/15MC/15ATH. The considerable exception was TPU/20MC/10AlPi, where the cotton was not ignited despite dripping, resulting in a non-flaming dripping V-0 classification. The main results relating to fire behaviour and flammability are summarized in Table 2. The most promising results were obtained when MC was combined with AlPi in TPU/20MC/10AlPi, so that this system was chosen for further investigation with other synergists/adjuvants in the later part of this paper.

3.1.3. Pyrolysis: mass loss and volatile products

The pyrolysis was analysed by TG coupled with FTIR (TG-FTIR) under nitrogen atmosphere. As reported in the literature [28–30], and corresponding well with the interpretation of the cone calorimeter results that TPU shows specific burning in two separate burning stages differing in terms of fuel, the thermal decomposition of polyurethanes occurred in two steps (Fig. 5 a). The DTG curves were separated in two groups (Fig. 5b and c) and the scale (x-axis) was increased for better readability. For easier comparison the TPU decomposition steps are denoted in Table 3 as $T_1/\Delta m_1$ and $T_3/\Delta m_3$. The middle step $T_2/\Delta m_2$ is associated with MC decomposition and was observed in flame-retarded systems where more than 10 wt.-% MC was used. Substantial decomposition in the TGA experiments is correlated to 5% loss is around 300 °C. Cleavage of the urethane groups in the hard segments occurred first. In the second step the soft segments decomposed, and as seen in the differential TG (DTG) curve (Fig. 5 b), the mass loss rate was around two times higher. Hardly any residue was left at the end of the test, which is consistent with observations made in the cone calorimeter. Addition of 10 wt.-% MC changed the decomposition, the decomposition steps were clearly separated, and Δm_1 and Δm_3 were nearly the same (Fig. 5 a, Table 3). The first step shifted slightly towards lower temperatures than for TPU (340 °C vs. 346 °C) as a result of MC interaction with TPU. For TPU/20MC and TPU/30MC the decomposition of MC appeared as a separate step (Fig. 5 a and b, $T_2/\Delta m_2$). It was noted that the mass loss was not constant and depended on the amount of MC used in a complex way. Assuming that this step is related purely to MC decomposition, in TPU/20MC the mass loss Δm_2 was about 12 wt.-%, which corresponds to around 60% of MC content, whereas for TPU/30MC it was 80% of MC. Further, the step corresponding to decomposition of the soft segments ($T_3/\Delta m_3$) shifted towards higher temperatures and the mass loss (Δm_3) was reduced, suggesting an inhibiting effect of the MC on the decomposition of TPU. The residue amount remaining after the test was comparable for TPU/10MC, TPU/20MC and TPU/30MC and reached around 5 wt.-%, in good agreement with the cone calorimeter results, considering that somewhat higher temperatures were reached in TG. It became clear that only a certain amount of MC shows interaction with the TPU, whereas an increasing amount of MC is released with increasing MC content. Thus, the pyrolysis of the TPU/MC materials explained well the fire behaviour in the cone calorimeter.

The TG and DTG curves of multicomponent systems are presented in Fig. 5 a and c, respectively. TPU/20MC/10AlPi showed a middle step, which is attributed to MC decomposition, but the mass loss at this step is higher than for TPU/20MC. Moreover, the last step attributed to soft segment decomposition was broader with a slight shoulder, and T_3 was shifted to 425 °C. Decomposition was influenced by AlPi and the release of pyrolysis products as well. TPU/15MC/15ATH started to decompose much earlier than the other materials, due to the early water release by ATH. The following steps took place earlier as well, indicating the interactions with the polymer matrix. At the end of the test 11 wt.-% residue remained in the crucible, which corresponds well with the cone calorimeter result. It was concluded that this inorganic residue is more thermally stable at higher temperatures than the residues of the other investigated materials, so that the residue yield shows no difference between TG and cone calorimeter.

To better understand the pyrolysis, the IR spectra of the evolved gases were monitored during the TG experiment; selected IR spectra are shown in Fig. 6. As indicated before, TPU decomposed in two steps. As the chain scission in TPU proceeded, signals from methylene diphenyl diisocyanate (MDI, 2278 cm^{-1}) and CO_2 (2359, 669 cm^{-1}) were observed in the spectrum and dominated. Additionally, tetrahydrofuran (THF, 2981–2870, 1082, 919 cm^{-1}) and

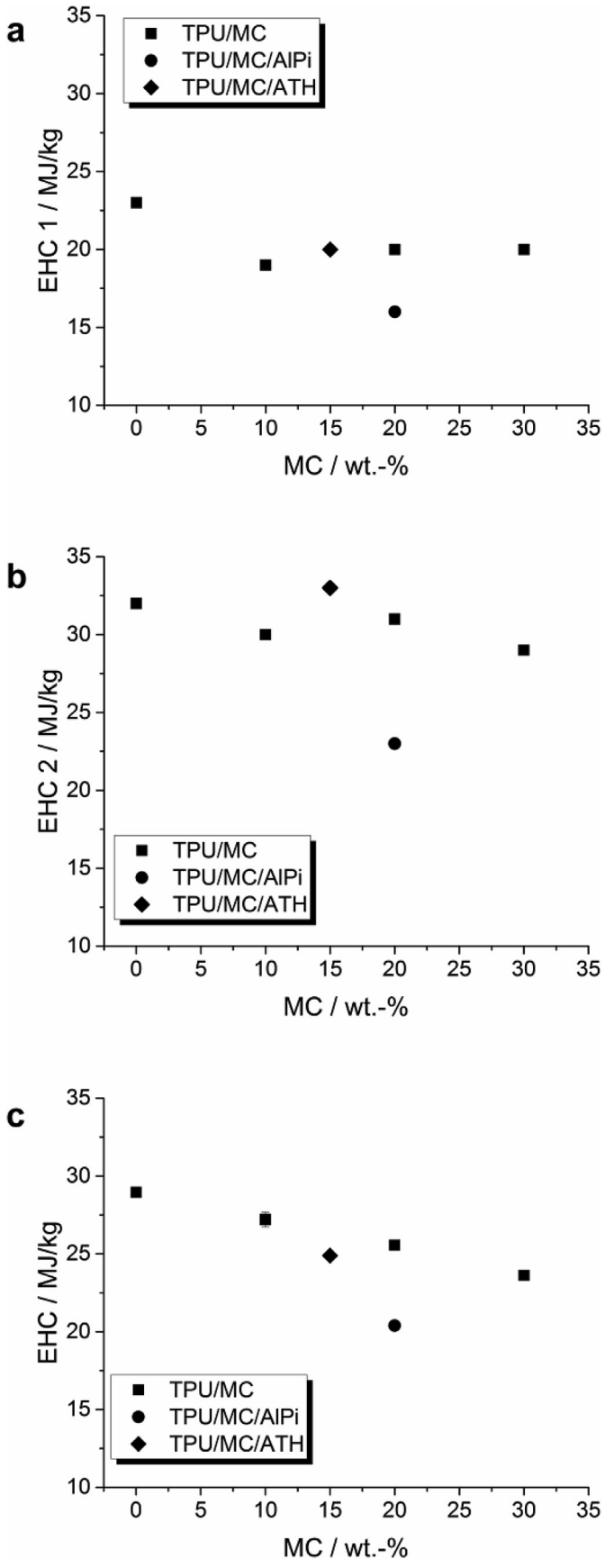

Fig. 3. EHC determined for the first EHC_1 (a) and the second EHC_2 (b) stage of burning, compared with EHC averaged over the entire burning time (c).

C=N groups (1522 cm^{-1}) were detected in the gas phase (Fig. 6 a). Later, at higher temperatures, more soft segments were decomposed and the main products were THF and CO_2 [30,31]. In the case of TPU/30MC, at first carbon dioxide was the main product evolved, along with some lower-intensity nitrogen groups. During the middle step (MC decomposition), ammonia (965, 930 cm^{-1}), and cyanic acid (3530, 2284, 2250 cm^{-1}) were detected (Fig. 6 b) [32]. Decomposition of MC is an endothermic process and acts as a heat sink, while the evolved gases cause fuel dilution. Thus, the evolved gas analysis explains well the improvement in performance in the cone calorimeter investigation. Towards the end of the decomposition mainly products of soft segment decomposition were identified. The gas-phase products originating from TPU/20MC/10AlPi pyrolysis (Fig. 6 c) were the same as in TPU/30MC throughout the measurement; however, additional signals were observed in the last step. Those signals are attributed to phosphinic acid (1152, 1087, 775 cm^{-1}), which is a typical product of AlPi decomposition observed in various materials [13,22,23,30,31].

The presence of ATH in TPU/15MC/15ATH caused increased water release, observed as multiple signals between 3918 and 3567 cm^{-1} and 1868-1396 cm^{-1} (Fig. 6 d). Moreover, the typical TPU decomposition products were no longer pronounced in the gas phase, so that mainly CO_2 was released. It is known that in some cases MDI may react further to form carbodiimides (N=C=N group). As an effect of the interactions with urethane groups during decomposition, a cross-linked structure may be formed [28]. This hypothesis explains the lack of strong MDI signals in the gas phase. There was only small shoulder visible on the CO_2 signal (2251 cm^{-1}), attributed to N=C=O bonds from MDI. MC products were not detected either, and only weaker bands of ammonia were observed. Those observations correspond well with the increased residue formation through interaction with the polymer matrix and the changed decomposition mechanism indicated by the shift in decomposition temperatures.

3.2. Multicomponent systems

The selection of multicomponent materials for the further applied investigation was built on the fundamental results presented above. The best fire performance was achieved when MC was combined with AlPi as a phosphorous flame retardant. To better understand the flame retardancy in TPU/MC/AlPi, as well as to further optimize performance, multicomponent systems were investigated using a third component such as MPP, varying the ratio between the additives, and introducing inorganic fillers as adjuvants. The results are compared with TPU and the commercial flame-retarded product TPU-FR. The materials discussed in the following section were all 2–2.1 mm thick and prepared by flat film extrusion.

3.2.1. Mechanical testing

In the applied research and development of the materials such as flame retarded TPU, both mechanical properties and fire performance have to be considered at the same time. Table 4 shows the measured elongation at break and tensile strength for all the samples. For comparison the values for TPU and TPU-FR are included. TPU showed the highest elongation at break, at 585%, and the commercial TPU-FR dropped 50% below the value of TPU. The TPU/18MC/5Clay compound was in a similar range as TPU-FR. The three compounds TPU/6MPP/9MC/15AlPi, TPU/15MC/15AlPi and TPU/6MPP/9MC/15AlPi/3Si were grouped around 400% elongation at break; TPU/10MC/10MPP even achieved 500%. The tensile strength showed some difference in the comparison of the compounds with each other. The compounds TPU/10MC/10MPP, TPU/15MC/15AlPi and TPU/6MPP/9MC/15AlPi/3Si had values slightly

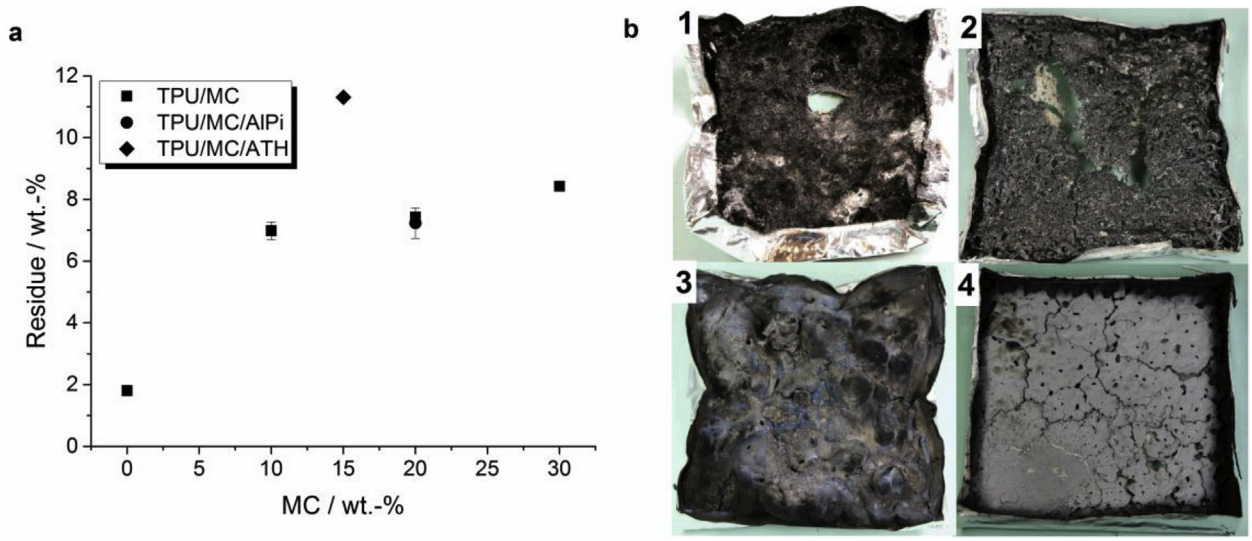

Fig. 4. Residue amount plotted over MC content (a) and pictures of the fire residues after the cone calorimeter tests (b): TPU (1), TPU/30MC (2), TPU/20MC/10AlPi (3) and TPU/15MC/15ATH (4).

above 20 MPa and therefore performed similarly to TPU-FR. The two compounds TPU/18MC/5Clay and TPU/6MPP/9MC/15AlPi were well over 30 MPa. The pure TPU material had a tensile strength of over 50 MPa. The addition of Si showed that the compound TPU/6MPP/9MC/15AlPi, which showed the best tensile strength compared to TPU, exhibited a strong decline in tensile strength. This decline was more powerful than the influence of Si in the elongation at break. The presented results showed that the content of AlPi, clay, and Si yields a significant decrease in elongation at break compared to pure TPU. In the results for tensile strength there was no precise tendency on the influence by the different additives. All of the investigated materials can compete with the commercial TPU-FR with respect to their mechanical properties.

3.2.2. *Screening the fire performance: rapid mass calorimeter (RMC)*

The RMC experiment indicated which materials might be of interest. By comparing the PHRR (Fig. 7 a) it was concluded that AlPi as a stand-alone additive in TPU/15AlPi is not efficient enough, resulting in the highest PHRR among flame-retarded systems. On the other hand, combining MC, AlPi and MPP caused a considerable reduction in PHRR compared to TPU. Plotting PHRR over THE (Fig. 7 b) shows the general tendency of the materials and can be used to assess performance. TPU/MC/Clay had the lowest PHRR, but because the curve was broader (i.e. the sample burned longer), it exhibited the highest THE of all materials. TPU/9MC/6MPP/15AlPi and TPU/9MC/6MPP/15AlPi/3Si performed similarly, indicating that the addition of silica had no influence on the result in the small scale. TPU-FR, as well as TPU/10MC/10MPP and TPU/15AlPi, showed similar THE values. TPU/15AlPi presented a rather high PHRR, but the strong flame-inhibiting effect of AlPi crucially reduced the THE. TPU/15MC/15AlPi showed the lowest THE, but the PHRR was slightly higher than when MC, MPP and AlPi were combined. The reason is the strong flame inhibition from AlPi, fuel dilution from MC (e.g. by ammonia release) and residue formation through the interaction of both. Replacing part of MC with MPP in TPU/9MC/6MPP/15AlPi yielded a higher total heat evolved due to the limited contribution of MPP to gas-phase activity, but the condensed-phase interaction and residue formation led to a crucial reduction in PHRR.

The closer look at the fire residues provides additional information about the flame retardancy going on in the condensed phase and also gives an idea of the interactions between additives in the condensed phase (Fig. 7 c). TPU (1) burns away completely and nearly no residue is formed, similar to TPU/15AlPi (3). TPU/10MC/10MPP (2) and TPU-FR (8) formed shiny, metallic residues coming mainly from MC, but MPP provided additional structure such that denser, more closed residue appeared. Introduction of clay led mostly to the development of inorganic ash with a rather closed and brittle surface (4). The residues of TPU/9MC/6MPP/15AlPi (5) and TPU/15MC/15AlPi (6) looked similar, indicating that a significant part of the residue evolved from MC-AlPi interaction. On the other hand, addition of silica to the three-additive system (7) provided residue support and yielded a smoother, more closed structure.

3.2.3. *Fire behaviour: cone calorimeter*

In the cone calorimeter, the shape of the HRR curves was much more pronounced than the RMC results and gave important insight into the fire behaviour of the materials investigated. For easier comparison, the results are presented in two plots (Fig. 8 a and b). A pronounced difference in time to ignition (t_{ig}) between TPU and flame-retarded samples was observed. For TPU (2 mm thick) the t_{ig} was similar to the 3-mm-thick TPU specimens investigated before (Fig. 2). TPU ignited after around 32 s. The introduction of the flame retardants caused interactions with the polymer matrix, however, and the effect on t_{ig} was more pronounced when the specimen was thinner. A worsening in t_{ig} occurred, which was not the case when 3-mm specimens were investigated. In Fig. 8 a TPU is compared with the system in which MC was combined with another additive. TPU/10MC/10MPP and TPU/18MC/5Clay showed a PHRR reduced from 2660 kW/m^2 to 639 and 627 kW/m^2 (Table 5), respectively. Furthermore, they showed a clear change in the HRR curve shape, which means that the burning behaviour of the material changed towards a char-forming type [24].

Closed-surface residue appeared, uniformly covering the aluminium tray in the case of TPU/10MC/10MPP (Fig. 8 c) and with some cracks for TPU/18MC/5Clay. MPP is a well-known flame retardant used in intumescent systems, which forms during the burning of highly cross-linked, phosphorus-rich char [35,36]. The organically modified clay, which is the basis for many nanocomposites, leads to the development of thermally stable

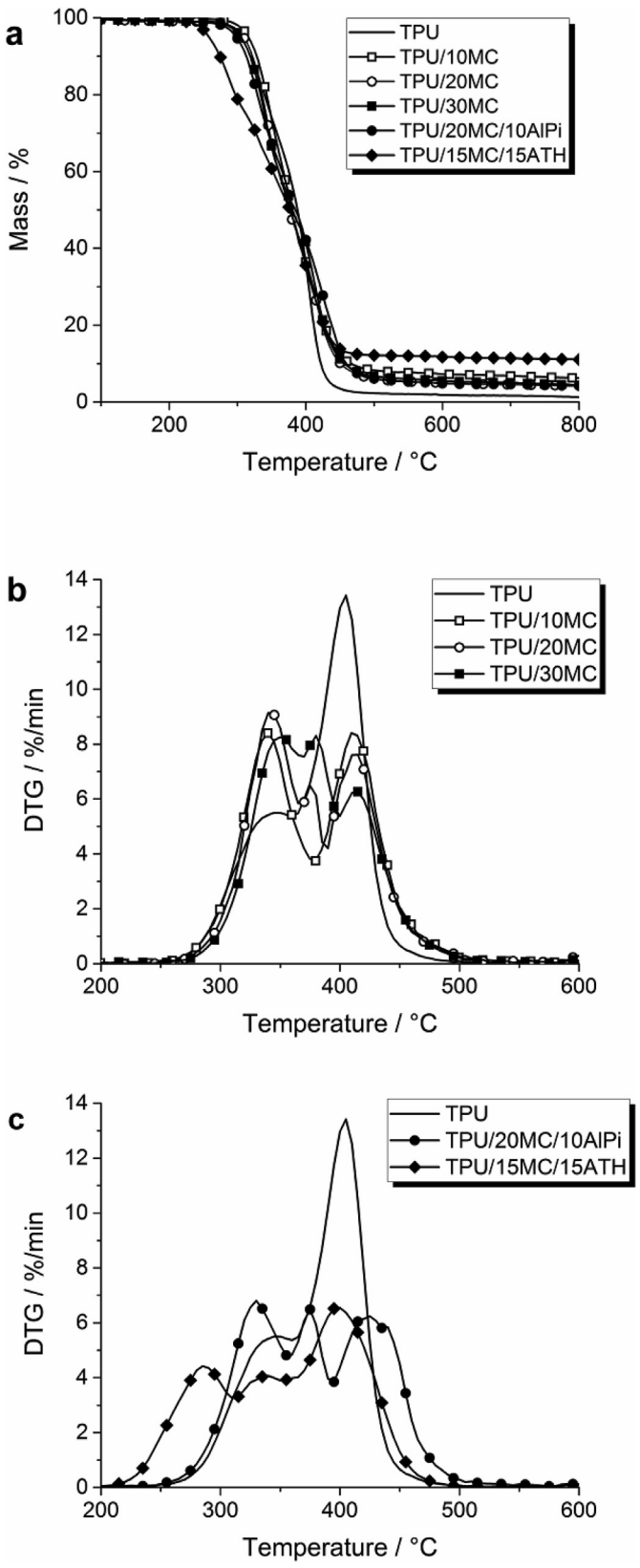

Fig. 5. Mass loss curves (a) and DTG for TPU, TPU/10MC, TPU/20 MC, TPU/30MC (b) and TPU, TPU/20MC/10AlPi, and TPU/15MC/15ATH (c).

inorganic-organic residue [37]. In the case of TPU/18MC/5Clay, the protective layer effect was reduced by the appearance of cracks [38]. TPU/15MC/15AlPi presented a PHRR of 834 kW/m^2, and the HRR curve shape typical for TPU was preserved. Nevertheless, similar to TPU/10MC/10MPP, the residue fully covered the aluminium tray and a uniformly closed surface was observed (Fig. 8c).

In Fig. 8 b the two multicomponent systems with the lowest PHRR are displayed along with the commercial product TPU-FR and TPU/15AlPi. The commercial product TPU-FR showed a slightly increased t_{ig}. The PHRR was rather high (1249 kW/m^2), but was reached later than in TPU. In addition, the characteristic shape observed for TPU remained. The residue showed the characteristic metallic shining noticed for materials containing MC and was very porous (Fig. 8 c). TPU-FR showed some improvements during initial burning, but a very disappointing flame-retardancy effect on the second burning stage as a liquid pool fire. In the case of TPU/15AlPi the characteristic HRR curve shape for TPU appeared as well, but the PHRR was significantly higher and reached 1755 kW/m^2. AlPi alone did not contribute much to condensed-phase reactions, so that residue formation was rather limited (Fig. 8 c), and overall it may be concluded that AlPi does not perform well as a stand-alone flame retardant in TPU, which is consistent with RMC results. The two best-performing materials were TPU/9MC/6MPP/15AlPi with a PHRR of 543 kW/m^2 and TPU/9MC/6MPP/15AlPi/3Si with a PHRR of 571 kW/m^2. Both materials displayed the HRR curve shape of charring-type materials without a pronounced peak. Without addition of silica the sample burned slightly longer, but the residue remaining after the test was rather loose and brittle (Fig. 8 c). When silica was mixed into the sample, additional stabilization of the residue occurred. The appearance of the residues of TPU/9MC/6MPP/15AlPi and TPU/9MC/6MPP/15AlPi/3Si indicated some specific interactions between MC—MPP—AlPi. The mixtures of MC and MPP and MC and AlPi led to the formation of a compact residue with a closed surface, whereas mixing MC with MPP and AlPi did not. There were blueish, shiny metallic parts in the residue of TPU/9MC/6MPP/15AlPi and TPU/9MC/6MPP/15AlPi/3Si, most probably coming from aluminium oxide. This means that incorporation of MC, MPP and AlPi in TPU changes the decomposition process, resulting in several additive-additive and/or additive-polymer interactions and yielding improved flame retardancy, even though no closed structure is formed. All of the cone calorimeter parameters are listed in Table 5.

In the flammability (reaction to small flame) test TPU/18MC/5Clay failed to achieve vertical UL 94 classification. The rest of the materials achieved V-2 classification. The TPU/20MC/10AlPi presented in the previous section achieved V-0 rating whereas TPU/15MC/15AlPi shown here reached V-2. Although those samples cannot be straightforwardly compared with each other due to the difference in the thickness, the main reason behind this phenomenon is most probably the levelling off effect of AlPi. Replacing part of MC with AlPi does not bring any further benefits and V-2 classification is reached. All samples extinguished very quickly, but the drops ignited the cotton. The exception was TPU-FR, where the drops did not ignite the cotton so that non-flaming dripping V-0 classification was achieved. The good UL 94 performance of TPU-FR may perhaps correspond somewhat to the initial burning in the cone calorimeter, but not to the entire HRR curve, to PHRR, or THE.

3.2.4. *Pyrolysis: mass loss and volatiles*

Table 6 summarizes the results obtained from TG. The experiments were conducted under nitrogen atmosphere to simulate anaerobic pyrolysis during burning. As observed in the cone calorimeter, specific interactions between MC, MPP, and AlPi led to improved flame retardancy; thus the mass, DTG and IR spectra for

Table 3
TG results. $T_{5\%}$ – temperature for 5% mass loss; $T_{1,2,3}$ – temperature for maximum mass loss rate at the 1st, 2nd and 3rd decomposition steps; $\Delta m_{1,2,3}$ – mass loss at 1st, 2nd and 3rd decomposition step. Residue mass taken at 800 °C.

Material	$T_{5\%}$ °C	T_1 °C	Δm_1 wt.-%	T_2 °C	Δm_2 wt.-%	T_3 °C	Δm_3 wt.-%	Residue wt.-%
TPU	305	346	31	–	–	404	68	1
TPU/10MC	308	340	47	–	–	412	46	5
TPU/20MC	309	342	44	375	12	411	39	5
TPU/30MC	313	351	42	384	21	412	32	5
TPU/20MC/10AlPi	300	329	36	374	17	425	42	4
TPU/15MC/15ATH	258	287	25	329	13	400	51	11

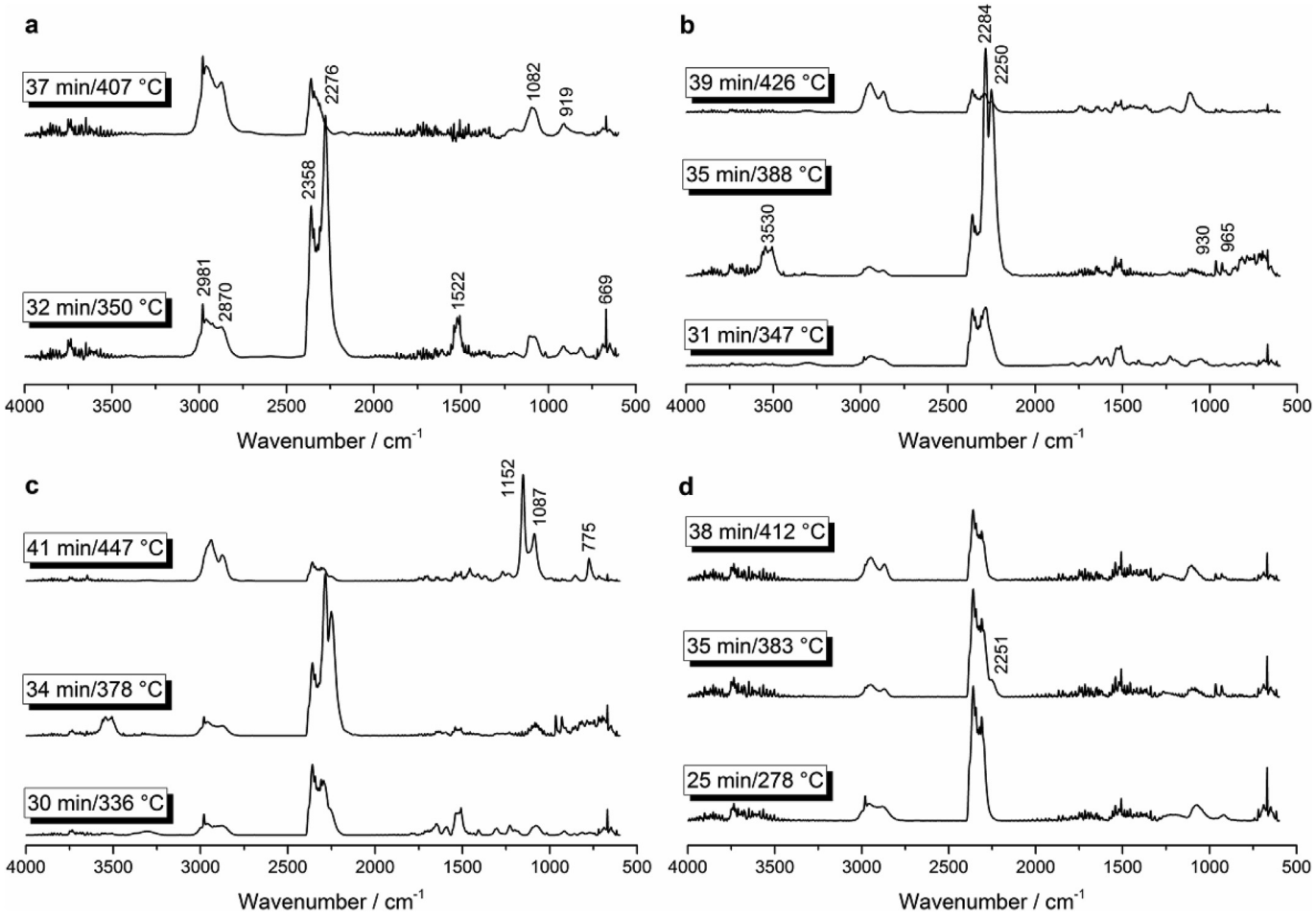

Fig. 6. IR spectra of selected materials: TPU (a), TPU/30MC (b), TPU/20MC/10AlPi (c) and TPU/15MC/15ATH (d).

Table 4
Elongation at break in % and tensile strength in MPa measured via quasi-static mechanical tests at a velocity of v = 100 mm/min using a universal tensile testing machine.

	Elongation at break/%	Tensile strength/MPa
TPU	585.5 ± 11.4	52.8 ± 1.2
TPU/10MC/10MPP	499.9 ± 10.1	38.6 ± 1.4
TPU/18MC/5Clay	326.8 ± 19.0	19.6 ± 1.2
TPU/6MPP/9MC/15AlPi	421.2 ± 4.8	25.7 ± 0.6
TPU/15MC/15AlPi	432.6 ± 29.3	24.8 ± 1.7
TPU/6MPP/9MC/15AlPi/3Si	388.3 ± 21.1	22.7 ± 0.9
TPU-FR	282.3 ± 3.4	21.4 ± 1.0

TPU/10MC/10MPP, TPU/15MC/15AlPi and TPU/9MC/6MPP/15AlPi are presented in Fig. 9 and analysed in detail.

Fig. 9 presents selected mass, DTG curves with corresponding IR spectra for each decomposition step. TPU/10MC/10MPP decomposed in two steps (Fig. 9 a). The maximum of the mass loss rate occurred at 342 °C, which was similar to the T_1 of TPU (346 °C), but the mass loss was higher (+22 wt.-%). The gas-phase products correspond to TPU decomposition, i.e. carbon dioxide (2360–2295, 669 cm^{-1}), tetrahydrofuran (2981–2874, 1078, 917 cm^{-1}) and C=N groups of melamine (1532 cm^{-1}). The second decomposition step shifted towards temperatures about 27 °C lower, and the mass lost was about 28 wt.-% lower than for TPU. During this step the main product in the gas phase was THF as a result of decomposition of the soft segments. A clear interaction between MC and TPU occurred, mainly enhancing the first decomposition step. Since the MC concentration was below 10 wt.-%, no additional MC step was observed.

In TPU/15MC/15AlPi (Fig. 9 b) the first decomposition step was shifted to temperatures about 20 °C lower than for TPU, but the

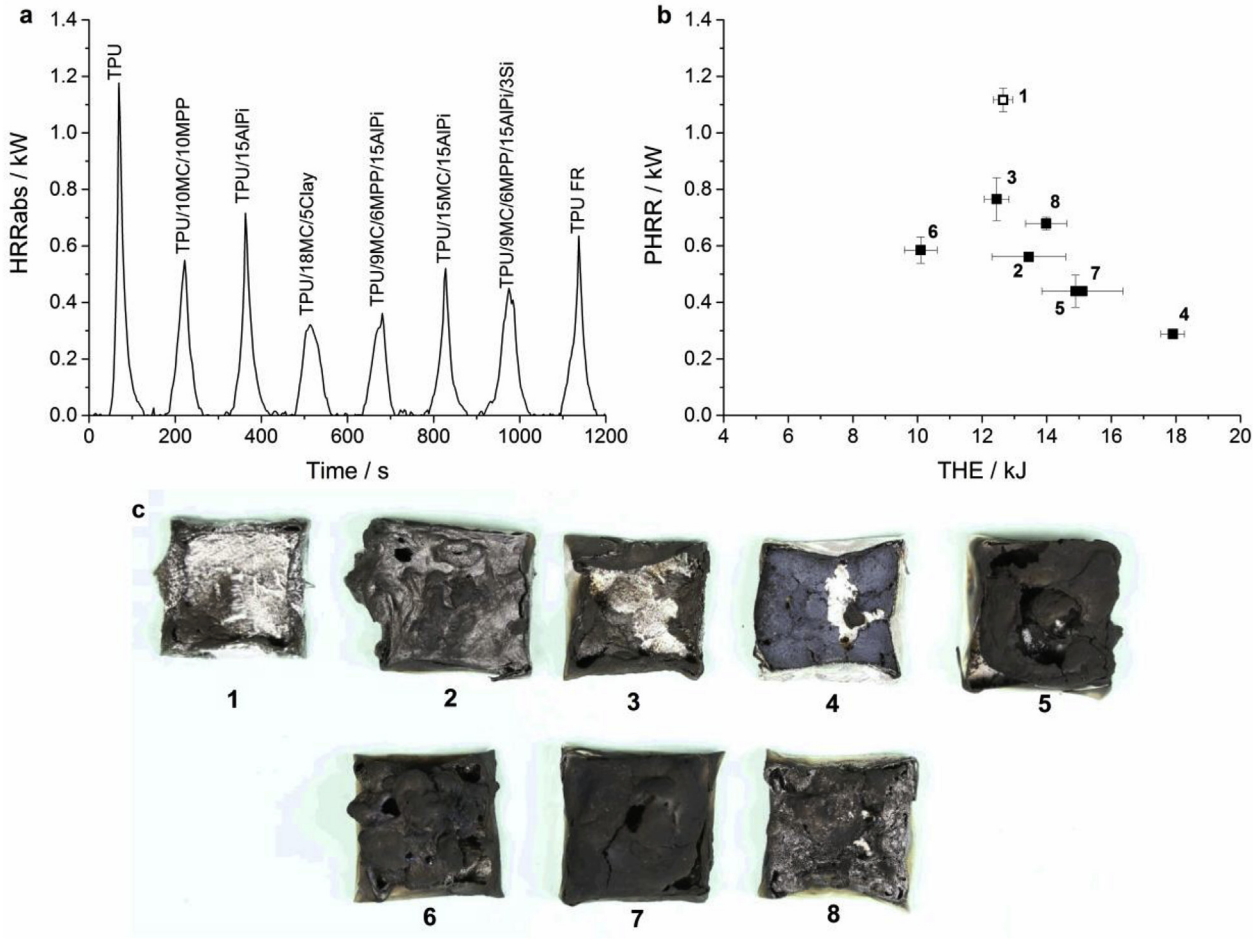

Fig. 7. RMC HRR curves for tested materials (a) and the assessment plotting PHRR over THE (b); residues after RMC test (c): TPU (1), TPU/10MC/10MPP (2), TPU/15AlPi (3), TPU/18MC/5Clay (4), TPU/9MC/6MPP/15AlPi (5), TPU/15MC/15AlPi (6), TPU/9MC/6MPP/15AlPi/3Si (7), TPU-FR (8).

mass loss was similar. The dominant IR signals identified were attributed to CO_2 and C=N groups. The THF was also detected, but the intensity was rather low compared with other materials investigated. The middle decomposition step was noticeable, with T_2 at 366 °C and a mass loss of 12 wt.-%, and was attributed to MC decomposition. The main products were cyanic acid (3545-3508 cm^{-1}), isocyanates (2286-2251 cm^{-1}), ammonia (965, 930 cm^{-1}) and carbon dioxide. In the last step, signals coming from phosphorus species, along with TPU decomposition products, were identified in the gas phase (1152, 1087, 775 cm^{-1}). These were volatiles released by AlPi decomposition to phosphinic acid [16,25,26,33,34].

Incorporation of all three additives in TPU, MC, MPP, and AlPi, resulted in changed decomposition (Fig. 9 c). Two decomposition steps were distinguished in DTG with a small shoulder at the second step. The T_1 shifted towards temperatures 15 °C lower than for TPU. During this step mainly the hard segments of TPU decomposed, and the IR evolved gas spectrum was dominated by CO_2 and nitrogen groups, with less intense THF signals. Additionally, P=N bonds were identified (1302, 1228 cm^{-1}), which were not as pronounced in other combinations [39]. In the second step, ammonia was released into the gas phase along with TPU pyrolysis products, but this occurred later than in TPU/15MC/15AlPi. Moreover, no signals from phosphinic acid were observed, but a strong ether band appeared (C–O–C, 1104 cm^{-1}). This clearly supported the statement about interactions between the additives and a changed decomposition mechanism. The multiple interactions are the mechanisms behind the improved performance in cone calorimeter test.

Among all of the materials investigated, only TPU/18MC/5Clay and TPU/15MC/15AlPi showed three steps, which is in good agreement with the observation that MC decomposition is not observed as a separate decomposition step when the concentration is below 10 wt.-%. The release of MC for those two materials was estimated at around 80%. The beginning of decomposition in TPU/18MC/5Clay ($T_{5\%}$) occurred noticeably earlier (around 290 °C) than in other formulations. It has been reported before that the incorporation of clay accelerates decomposition due to the catalysis of polymer degradation and early breakdown of the filler itself [7].

TPU-FR showed one major decomposition step at 356 °C with a mass loss of 94 wt.-%. A small shoulder was detected, most probably corresponding to the second decomposition process of TPU, but it was not considered as a separate step in TPU-FR. This means that all decomposition processes merged into a single step with a very high mass loss rate as a result of polymer-additive interaction. The TG results, similar to the cone calorimeter results of TPU-FR, did not indicate a high flame-retardancy efficiency of TPU-FR in UL 94. The residues taken at 800 °C corresponded well with the observations in the cone calorimeter.

3.2.5. *Assessing the fire hazard: Petrella plot*

The Petrella plot was introduced in the early 1990s as a visual

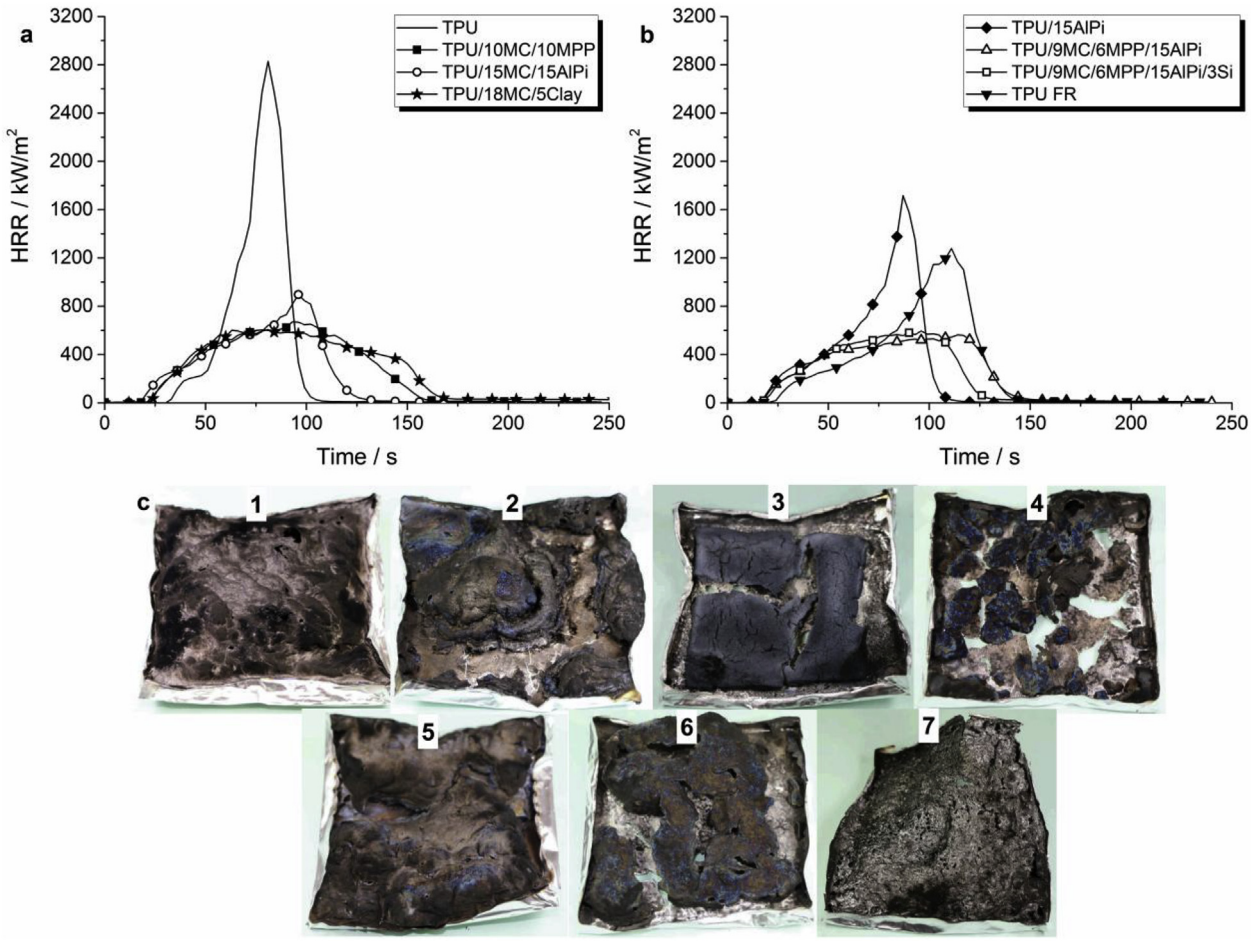

Fig. 8. HRR curves obtained in the cone calorimeter for multicomponent mixtures (a) and (b); residues after cone calorimeter test (c): TPU/10MC/10MPP (1), TPU/15AlPi (2), TPU/18MC/5Clay (3), TPU/9MC/6MPP/15AlPi (4), TPU/15MC/15AlPi (5), TPU/9MC/6MPP/15AlPi/3Si (6), TPU-FR (7).

Table 5
Cone calorimeter data. PHRR – peak heat release rate; THE – total heat evolved; EHC – effective heat of combustion.

Name	PHRR kW/m^2	THE MJ/m^2	EHC MJ/kg	Residue %	UL 94 Vertical
TPU (2 mm)	2660	66	31	3	–
TPU/10MC/10MPP	639	58	23	7	V-2
TPU/15AlPi	1755	58	22	2	V-2
TPU/18MC/5Clay	627	60	25	10	N/R
TPU/9MC/6MPP/15AlPi	543	48	19	6	V-2
TPU/15MC/15AlPi	834	48	20	4	V-2
TPU/9MC/6MPP/15AlPi/3Si	571	44	20	8	V-2
TPU-FR	1249	61	20	5	V-0

Table 6
TG results. $T_{5\%}$ – temperature for 5% mass loss; $T_{1,2,3}$ – temperature for maximum mass loss rate at 1st, 2nd and 3rd decomposition step; $\Delta m_{1,2,3}$ – mass loss at 1st, 2nd and 3rd decomposition step. Residue mass taken at 800 °C.

Name	$T_{5\%}$ °C	T_1 °C	Δm_1 %	T_2 °C	Δm_2 %	T_3 °C	Δm_3 %	Residue %
TPU	305	346	31	–	–	404	68	1
TPU/10MC/10MPP	307	342	53	–	–	377	40	7
TPU/15AlPi	301	322	42	–	–	419	55	3
TPU/18MC/5Clay	291	336	42	373	15	418	33	8
TPU/9MC/6MPP/15AlPi	299	331	41	–	–	419	51	8
TPU/15MC/15AlPi	300	326	35	366	12	429	48	4
TPU/9MC/6MPP/15AlPi/3Si	300	329	40	–	–	413	51	9
TPU-FR	313	356	94	–	–	–	–	6

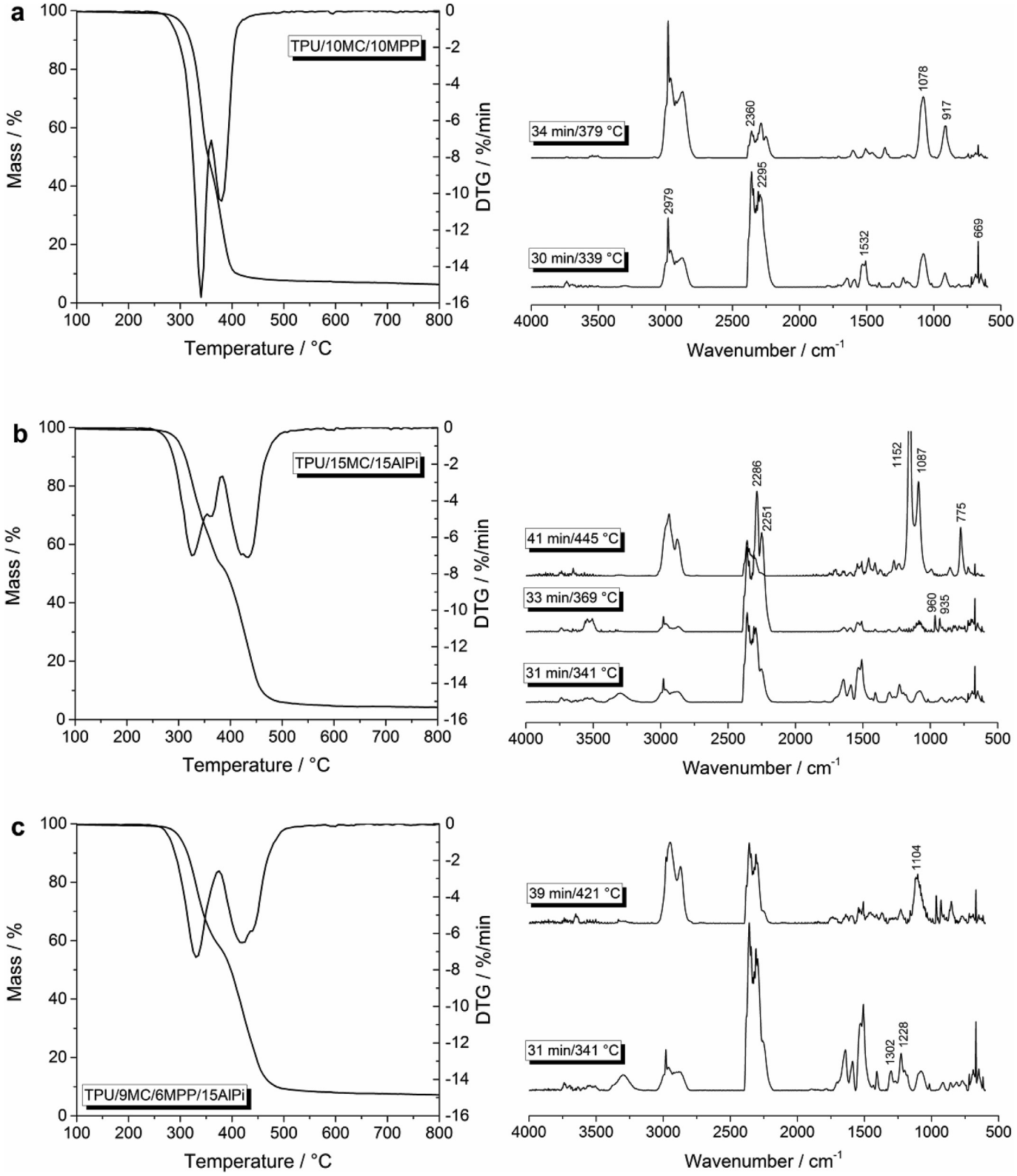

Fig. 9. TG-FTIR results: Selected mass, DTG with corresponding IR spectra typical for the decomposition steps of TPU/10MC/10MPP (a), TPU/15MC/15AlPi (b) and TPU/9MC/6MPP/15AlPi (c).

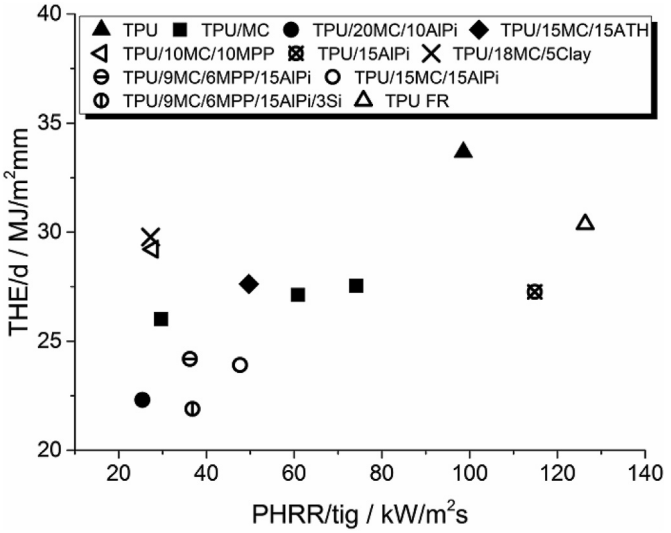

Fig. 10. Petrella-like plot including all tested materials.

tool for assessing the fire hazard of materials by plotting the total heat evolved (THE) against an index for flame spread ($PHRR/t_{ig}$) [40]. Fig. 10 presents a Petrella-like graphical assessment for all of the materials investigated. Since two different thicknesses (d) were used, the normalized specific THE/d replaced the absolute fire load in Fig. 10. Several groups of materials were distinguished in the plot. TPU (closed triangle) showed the highest THE/d value, but because t_{ig} was relatively long compared to some of the other investigated materials, the $PHRR/t_{ig}$ parameter was moderately high. TPU/15AlPi (crossed circle) and TPU-FR (open triangle) had lower PHRR than TPU, but much shorter times to ignition, so they appear further to the right of the plot. The THE was reduced, but the flame spread factor was higher. It is worth noting that the TPU-FR, exhibiting non-flaming dripping V-0, does not show any convincing flame retardancy effect in the cone calorimeter.

TPU/10MC/10MPP (slanted open triangles) and TPU/18MC/5Clay (crosses) are two examples where the flame-spread parameter was reduced significantly, but neither MPP nor clay contribute to gas-phase or charring activity to reduce the THE. TPU/10MC and TPU/20MC (closed squares) as well as TPU/15MC/15ATH (closed diamonds) presented similar THE values and t_{ig}, but differed in PHRR, so the lowest $PHRR/t_{ig}$ was observed for TPU/15MC/15ATH. The fire behaviour of TPU/30MC was changed and a lower fire hazard was observed. Below 30 wt.-% of MC no significant improvement in fire performance of TPU/MC occurred. All of the multicomponent materials with AlPi presented the best flame retardancy and were located closest to the origin of the plot. At this point it should be noted that the thickness of the specimen plays a significant role; although it was taken into account in THE/d, its influence on t_{ig} is crucial as well, but was not evaluated as straightforwardly as for THE. This explains why TPU/20MC/10AlPi (closed circles) is closer to the origin of the plot than multicomponent systems, even though the PHRR was reduced more strongly in the latter. Nevertheless, it is clear that the combination of MC with AlPi and alternative additional flame retardants yields the best performance while maintaining relatively low additive concentrations, i.e. no more than 30 wt.-%.

3.2.6. Correlations

To directly compare the accelerated fire testing method RMC and the cone calorimeter, the correlation coefficients between

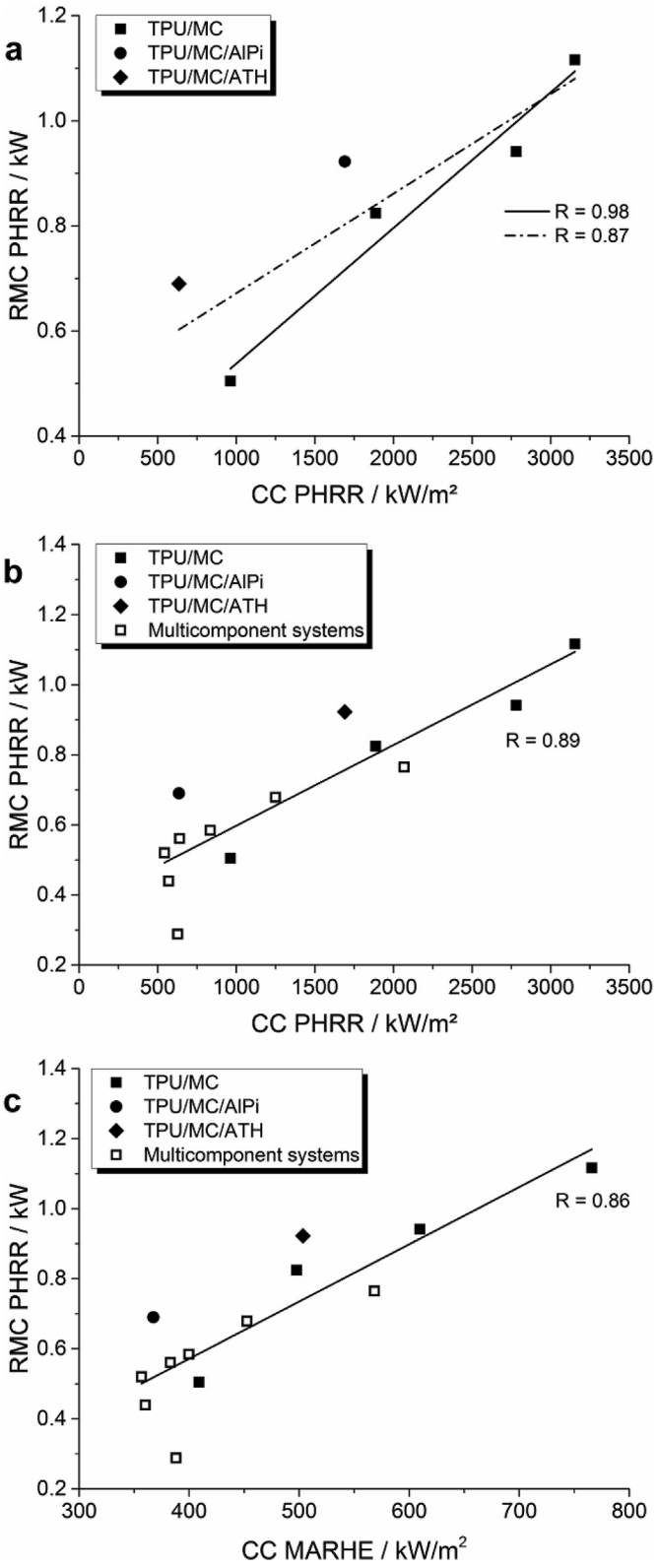

Fig. 11. Correlation between PHHR measured with RMC and cone calorimeter for TPU/MC, TPU/MC/AlPi, and TPU/MC/ATH (a); the dashed-dotted line represents the correlation over all points, the solid line the correlation for the MC materials. Correlation between RMC PHRR and cone calorimeter PHRR (a) and MARHE (b) for all materials tested.

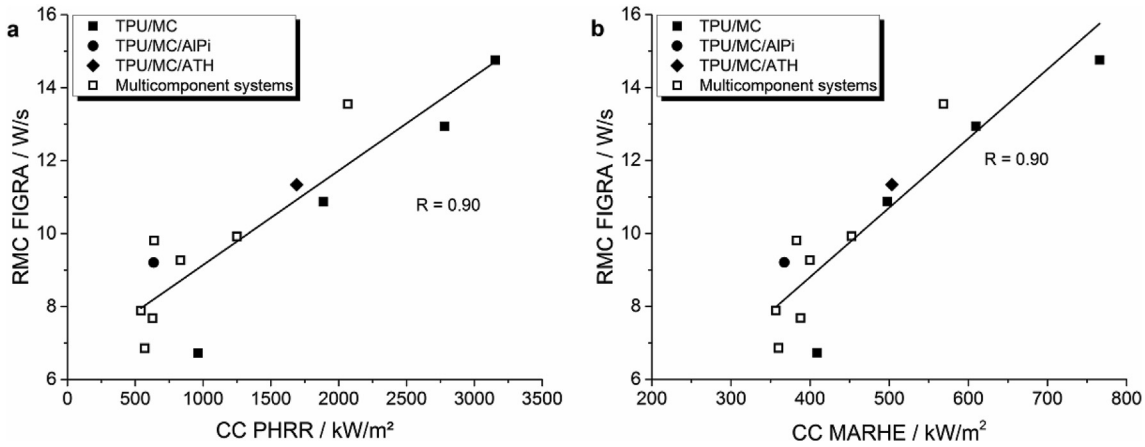

Fig. 12. Correlations between RMC FIGRA and cone calorimeter PHRR (a) and MARHE (b) for all tested materials.

several of their results were evaluated. PHRR was one of the characteristics that correlated strongly and was highly reliable. As seen in Fig. 11a, the R coefficient reached 0.98 when only the variation in the MC concentration was considered (Fig. 11, solid line). Combining MC with AlPi or ATH in TPU/MC/AlPi and TPU/MC/ATH, and thus changing the flame-retardancy modes of action, led to higher deviation. Nevertheless, when TPU/MC (10, 20 and 30 wt.-%) was considered together with TPU/20MC/10AlPi and TPU/15MC/15ATH, the correlation remains strong (R = 0.87, dashed-dotted line).

Since PHRR from the RMC test was established as a reliable parameter, it was compared with several other characteristics from cone calorimeter (Fig. 11 b and c). All investigated materials with a thickness of 2 or 3 mm are presented. Considering PHRR values from both methods, the correlation remained quite strong (R = 0.89). This means that reduction in specimen size does not result in a loss of information about the flame-retarding effects and reduction in PHRR. Strong correlations were also observed between PHRR measured in RMC and MARHE (maximum average rate of heat emission) from the cone calorimeter (R = 0.86, Fig. 11 c). MARHE represents a somewhat averaged HRR curve and can be compared directly with the single PHRR in RMC, which also depicts a kind of average. In both cases the correlation would be even stronger if the TPU/MC/Clay were not taken into account. Due to the different kind of flame-retardant mechanism in nanocomposites compared to the other rather traditional flame retardants, TPU/18MC/5Clay behaves as an outlier.

Not only PHRR (RMC) showed good agreement with PHRR or MARHE from the cone calorimeter. When FIGRA (fire growth rate) was considered, an even stronger R coefficient was observed (0.90) (Fig. 12). This is because FIGRA is directly related to the slope of the HRR curve. Since the curve in RMC is represented mostly as a peak without major features, FIGRA correlates strongly with PHRR. This happens analogously in the case of correlation between FIGRA and MARHE.

4. Conclusions

A comprehensive multi-methodical study on flame-retarded TPU systems was presented. A special focus was on RMC as an accelerated screening method. MC is not very effective for contents below 30 wt.-%, and the flame-retardancy efficiency may level off before reaching sufficiently flame-retardant properties. When MC was combined with AlPi the results were significantly improved, leading to reduction in PHRR in the cone calorimeter from 3154 kW/m^2 to 635 kW/m^2, and V-0 classification in the UL 94 test. A detailed evaluation of EHC was presented, based on the assumption that two burning stages are observed in the cone calorimeter with very different EHC. The analysis revealed that the first stage corresponds mainly to decomposition of the hard segments, and the second stage mainly to the soft segment decomposition, yielding a liquid pool fire in the cone calorimeter. The strongest influence on EHC in both stages was observed for TPU/20MC/10AlPi, which is explained by the strong flame-inhibiting effect of AlPi together with fuel dilution provided by MC.

The analysis of multicomponent systems showed that combining MC, AlPi and MPP leads to the most promising results as far as the cone calorimeter data are considered. In the cone calorimeter the PHRR was reduced to 543 kW/m^2. In the UL 94 test V-2 classification was reached, the samples extinguished within few seconds, and only a few drops were formed. The interplay of MC, MPP and AlPi led to a changed decomposition mechanism observed in TG-FTIR.

The reliability of RMC was confirmed by correlation experiments. Several strongly correlating parameters between RMC and cone calorimeter were found. Based on these it is possible to predict the performance in the cone calorimeter based on the RMC. The RMC can be used successfully for screening to identify well-performing materials in terms of fire behaviour. The reliability seems to be limited when different flame-retardancy modes of action occur, particularly with respect to quite specific performance in various fire tests, such as the non-flaming dripping V-0 in UL 94 that was clearly met by TPU/20MC/10AlPi, but not TPU-FR.

Funding

The IGF Project (19078 N/2) of the Research Association was supported by the Arbeitsgemeinschaft industrieller Forschungsvereinigungen (AiF) within the framework of the program “Förderung der Industriellen Gemeinschaftsforschung (IGF)” of the German Federal Ministry for Economic Affairs and Energy based on a decision of the Deutschen Bundestag.

References

[1] J.G. Drobny, in: Handbook of Thermoplastic Elastomers, second ed., Elsevier, Oxford, UK, 2014. PDL Handbook Series.
[2] C. Hepburn, in: Polyurethane Elastomers, second ed., Elsevier Applied Science, London, UK, 1991.
[3] Z. Wirpsza, Polyurethanes: Chemistry, Technology and Applications, Series: Polymer Science and Technology, Ellis Horwood Ltd., New York, USA, 1993.
[4] M. Szycher, in: Szycher's Handook of Polyurethanes, second ed., CRC press,

Boca Raton, 2013.
[5] T. Engelmann, A. Luks, O. Töpfer, R. Sauerwein (Eds.), New Aluminium Hydrates as Flame Retardant Fillers for TPU. 61st International Wire & Cable Symposium, 2012 (Providence, RI, USA).
[6] X. Chen, C. Ma, C. Jiao, Synergistic effects between iron-graphene and ammonium polyphosphate in flame-retardant thermoplastic polyurethane, J. Therm. Anal. Calorim. 126 (2016) 633–642.
[7] D. Tabuani, F. Bellucci, A. Terenzi, G. Camino, Flame retarded thermoplastic polyurethane (TPU) for cable jacketing application, Polym. Degrad. Stabil. 97 (2012) 2594–2601.
[8] U.A. Pinto, L.L.Y. Visconte, R.C.R. Nunes, Mechanical properties of thermoplastic polyurethane elastomers with mica and aluminum trihydrate, Eur. Polym. J. 37 (2001) 1935–1937.
[9] M. Lin, B. Li, Q. Li, S. Li, S. Zhang, Synergistic effect of metal oxides on the flame retardancy and thermal degradation of novel intumescent flame-retardant thermoplastic polyurethanes, J. Appl. Polym. Sci. 121 (2010) 1951–1960.
[10] M. Bugajny, M. Le Bras, S. Bourbigot, Short communication: new approach to the dynamic properties of an intumescent material, Fire Mater. 23 (1999) 49–51.
[11] R.E. Myers, E.D.J. Dickens, E. Licursi, R.E. Evans, Ammonium pentaborate: an intumescent flame retardant for thermoplastic polyurethanes, J. Fire Sci. 3 (1985) 432–449.
[12] S.V. Levchik, E.D. Weil, Thermal decomposition, combustion and fire-retardancy of polyurethanes – a review of the recent literature, Polym. Int. 53 (2004) 1585–1610.
[13] A. Toldy, G. Harakály, B. Szolnoki, E. Zimonyi, G. Marosi, Polym. Degrad. Stabil. 97 (2012) 2524–2530.
[14] Eckstein Y, Hewitt LE, Fudala BB. Flame Retardant Thermoplastic Polyurethane Containing Melamine Cyanurate. Google Patents; 2004.
[15] H. Li, N. Ning, L. Zhang, Y. Wang, W. Liang, Different flame retardancy effects and mechanisms of aluminium phosphinate in PPO, TPU and PP, Polym. Degrad. Stabil. 105 (2014) 86–95.
[16] K. Langfeld, A. Wilke, A. Sut, S. Greiser, B. Ulmer, V. Andrievici, P. Limbach, M. Bastian, B. Schartel, Halogen-free fire retardant styrene-ethylene-butylene-styrene-based thermoplastic elastomers using synergistic aluminium diethylphosphinate-based combinations, J. Fire Sci. 33 (2015) 157–177.
[17] B. Schartel, B. Perret, B. Dittrich, M. Ciesielski, J. Krämer, P. Müller, V. Altstädt, L. Zang, M. Döring, Flame retardancy of polymers: the role of specific reactions in the condensed phase, Macromol. Mater. Eng. 301 (2016) 9–35.
[18] B. Schartel, K.H. Pawlowski, R.E. Lyon, Pyrolysis combustion flow calorimeter: a tool to assess flame retarded PC/ABS materials? Thermochim. Acta 462 (2007) 1–14.
[19] R.E. Lyon, R.N. Walters, Pyrolysis combustion flow calorimetry, J. Anal. Appl. Pyrolysis 71 (2004) 27–46.
[20] S. Rabe, B. Schartel, The rapid mass calorimeter: understanding reduced-scale fire test results, Polym. Test. 57 (2017) 165–174.
[21] S. Rabe, B. Schartel, The rapid mass calorimeter: a route to high throughput fire testing, Fire Mater. 41 (2017) 834–847.
[22] B. Schartel, M. Bartholmai, U. Knoll, Some comments on the use of cone calorimeter data, Polym. Degrad. Stabil. 88 (2005) 540–547.
[23] L.L. Havlicek, R.D. Crane, Practical Statistics for the Physical Sciences, American Chemical Society, Washington, DC, 1988.
[24] B. Schartel, T.R. Hull, Development of fire-retarded materials – interpretation of cone calorimeter data, Fire Mater. 31 (2007) 327–354.
[25] S. Brehme, T. Köppl, B. Schartel, V. Altstädt, Competition in aluminium phosphinate-based halogen-free flame retardancy of poly(butylene terephthalate) and its glass-fibre composites, E-polymers 14 (3) (2014) 193–208.
[26] S. Brehme, B. Schartel, J. Goebbels, O. Fischer, D. Pospiech, Y. Bykov, M. Döring, Phosphorus polyester versus aluminium phosphinate in poly(butylene terephtalate) (PBT): flame retardancy performance and mechanisms, Polym. Degrad. Stabil. 96 (2011) 875–884.
[27] W. Yang, L. Song, Y. Hu, H. Lu, R.K.K. Yuen, Enhancement of fire retardancy performance of glass-fibre reinforced poly(ethylene terephthalate) composites with the incorporation of aluminum hypophosphite and melamine cyanurate, Composites Part B 42 (2011) 1057–1065.
[28] D.K. Chattopadhyay, D.C. Webster, Thermal stability and flame retardancy of polyurethanes, Prog. Polym. Sci. 34 (2009) 1068–1133.
[29] N. Grassie, G.A. Perdomo Mendoza, Thermal degradation of polyether-urethanes: 5. Polyether-urethanes prepared from methylene bis(4-phenylisocyanate) and high molecular weight poly(ethylene glycols) and the effect of ammonium polyphosphate, Polym. Degrad. Stabil. 11 (4) (1985) 359–379.
[30] M. Herrera, G. Matuschek, A. Kettrup, Thermal degradation of thermoplastic polyurethane elastomers (TPU) based on MDI, Polym. Degrad. Stabil. 78 (2002) 323–331.
[31] B. Stuart, Infrared Spectroscopy: Fundamentals and Applications. Analytical Techniques in the Sciences, John Wiley & Sons, Ltd., 2004.
[32] U. Braun, B. Schartel, Flame retardancy mechanisms of aluminium phosphinate in combination with melamine cyanurate in glass-fibre-reinforced poly(1,4-butylene terephthalate), Macromol. Mater. Eng. 293 (2008) 206–217.
[33] A. Sut, S. Greiser, C. Jäger, B. Schartel, Aluminium diethylphosphinate versus ammonium polyphosphate: a comprehensive comparison of the chemical interactions during pyrolysis in flame-retarded polyolefine/poly(phenylene oxide), Thermochim. Acta 640 (2016) 74–84, https://doi.org/10.1016/j.tca.2016.08.004.
[34] U. Braun, H. Bahr, H. Sturm, B. Schartel, Flame retardancy mechanisms of metal phosphinates and metal phosphinates in combination with melamine cyanurate in glass-fiber reinforced poly(1,4-butylene terephthalate): the influence of metal cation, Polym. Adv. Technol. 19 (2008) 680–692.
[35] U. Braun, B. Schartel, M.A. Fichera, C. Jäger, Flame retardancy mechanisms of aluminium phosphinate in combination with melamine polyphosphate and zinc borate in glass-fibre reinforced polyamide 6,6, Polym. Degrad. Stabil. 92 (2007) 1528–1545.
[36] P. Müller, M. Morys, A. Sut, C. Jäger, B. Illerhaus, B. Schartel, Melamine poly(zinc phosphate) as flame retardant in epoxy resin: decomposition pathways, molecular mechanisms and morphology of fire residues, Polym. Degrad. Stabil. 130 (2016) 307–319, https://doi.org/10.1016/j.polymdegradstab.2016.06.023.
[37] B. Schartel, A. Weiß, H. Sturm, M. Kleemeier, A. Hartwig, C. Vogt, R.X. Fischer, Layered silicate epoxy nanocomposites: formation of the inorganic-carbonaceous fire protection layer, Polym. Adv. Technol. 22 (2011) 1581–1592.
[38] G.M. Wu, B. Schartel, M. Kleemeier, A. Hartwig, Fire behavior of layered silicate epoxy nanocomposites combined with low-melting inorganic ceepree glass, Polym. Eng. Sci. 52 (2012) 507–517.
[39] H.R. Allcock, Phosphorus-nitrogen Compounds. Cyclic, Linear, and High Polymeric Systems, Academic Press, New York, USA, 1972.
[40] R.V. Petrella, The assessment of full-scale fire hazards from cone calorimeter data, J. Fire Sci. 12 (1994) 14–43.